10 Radiomagnetotellurics

Bülent Tezkan

10.1 Introduction

The application of geophysical techniques to hydrogeological questions has grown in importance due to the increasing concern of environmental issues. Electric and electromagnetic (EM) methods are the most important geophysical techniques for groundwater studies (Nobes 1996) and they are also frequently used for the characterisation of shallow structures. General discussions on the use of EM techniques for shallow geophysical applications and especially for groundwater studies can be found in Mc Neill (1990); Nobes (1996); Tezkan (1999); Pellerin (2002) and Bechtel et al. (2007). In order to derive the subsurface lithology (e.g. groundwater permeable and impermeable layers) the conductivity is used as a petrophysical parameter which is sensitive to the variation of porosity, the water saturation, the conductivity of the pore fluid and the clay content. The radiomagnetotelluric method is a relatively new technique of applied electromagnetic geophysics and is extensively used in connection with near surface exploration (Turberg and Barker 1999, Linde and Pedersen 2004, Tezkan et al. 2005). It uses military and civilian radio transmitters broadcasting in the frequency range between 10 kHz and 1 MHz. The high frequency range allows to study the shallow subsurface using inversion items originally developed for magnetotelluric data (Smith and Booker 1991, Mackie et al. 1997, Siripunvarapon and Egbert 2000). The shallow investigation depth makes it easier for the interpreter to constrain and correlate resistivity models with available prior information such as borehole data and hydraulic tests at different scales (Linde and Pedersen 2004). The RMT technique has also been used successfully to delimit waste sites (Tezkan et al. 2000, 2005; Newman et al. 2003) using 2D and 3D inversion techniques. (Turberg et al. 1994) showed the estimation of the lithological inhomogenity using RMT data. Linde and Pedersen (2004) demonstrated the application of the RMT-method to characterize fractured granite and to define the direction and magnitude of electrical anisotropy of a limestone formation. Several successful applications of this method concerning aquifer characterisations have been also reported in the literature.

10.2 Basic principles of the RMT – method

The sources employed in this method are remote radio transmitters which provide electromagnetic plane waves with frequencies between 10 kHz and 1 MHz. The frequency dependent apparent resistivity and phase curves can be obtained by measuring the components of the electric and magnetic field at the surface. In order to calculate them, and to describe the radiomagnetotelluric wave propagation, the basic wave propagation theory of electromagnetics should be considered. Maxwell's equations are used to understand the propagation and attenuation of such waves.

A detailed description of the theory can be found in Nabighian (1987) and Telford et al. (1990). Assuming the electric charge density q = 0, the Maxwell equation is given by:

$$\nabla \times \vec{E} + \frac{\partial \vec{B}}{\partial t} = 0 \tag{10.1}$$

$$\nabla \times \vec{H} = \vec{J} + \frac{\partial \vec{D}}{\partial t} \tag{10.2}$$

$$\nabla \cdot \vec{B} = 0 \tag{10.3}$$

$$\nabla \cdot \vec{E} = 0 \tag{10.4}$$

where J is the current density (A/m²), E = electric field intensity (V/m), B = magnetic flux density (Vs / m²), H = magnetic field intensity (A/m) and D = electric displacement (C/m²). Furthermore, the material equations in a homogeneous, isotropic media are valid:

$$\vec{B} = \mu \cdot \vec{H} \tag{10.5}$$

$$\vec{D} = \varepsilon \cdot \vec{E} \tag{10.6}$$

$$\vec{J} = \sigma \cdot \vec{E}$$

where σ is the electric conductivity (S/m), μ is the magnetic permeability, (Vs/Am) and ε the dielectric capacity (As/Vm). Taking the curl of Eq. 10.1 and 10.2 by considering Eq. 10.6 we get:

$$\nabla^2\vec{E} = \mu\sigma\frac{\partial\vec{E}}{\partial t} + \mu\varepsilon\frac{\partial^2\vec{E}}{\partial t^2} \tag{10.7}$$

$$\nabla^2\vec{H} = \mu\sigma\frac{\partial\vec{H}}{\partial t} + \mu\varepsilon\frac{\partial^2\vec{H}}{\partial t^2}$$

by using the vector identity:

$$\nabla\times\left(\nabla\times\vec{a}\right) = \nabla\left(\nabla.\vec{a}\right) - \nabla^2\vec{a} \tag{10.8}$$

In problems involving fields varying with time, the introduction of the general harmonic function simplifies the analysis:

$$\vec{F} = \vec{F}_0 \cdot e^{i\omega t} \tag{10.9}$$

$$\text{with } \vec{F} \in \{\vec{E}, \vec{H}\}, \vec{F}_0 \in \{\vec{E}_0, \vec{H}_0\}.$$

Upon substitution of this type of time dependency in Eq. 10.7 we get:

$$\nabla^2\vec{F} = i\omega\mu\vec{F} - \omega^2\mu\varepsilon\vec{F} \tag{10.10}$$

$$\text{with } \vec{F} \in \{\vec{E}, \vec{H}\}$$

The first and the second term on the right hand side are related to the conductivity and displacement currents respectively. Eq. 10.10 also describes the propagation of the magnetic and electric field vectors in an isotropic homogenous medium. Displacement currents can be neglected for the RMT frequencies (10 kHz - 1 MHz) used for normal resistivity distributions (eg. $\rho < 500\ \Omega m$). In this case, the well developed and tested magnetotelluric interpretation software (1D - 2D inversion of the data) is used to derive the conductivity distribution of the subsurface. As a result we have:

$$\nabla^2\vec{F} - k^2\vec{F} = 0 \tag{10.11}$$

with $k^2=i\omega\mu\sigma$

However, for the application of this method on crystalline environments the displacement currents must be taken into account (Persson and Pedersen 2002). Conductivity distribution of the subsurface should be considered in order to solve Eq. 10.11. The easiest case is the homogenous half space and 1D conductivity distribution, e.g. that the conductivity varies only in z direction (positive to the direction from the surface down to the earth). This means, that all the variations in horizontal direction, also in the x - y direction are zero.

$$\frac{\partial F_j}{\partial x} = \frac{\partial F_j}{\partial y} = 0$$

Eq. 10.11 can then be written by:

$$\frac{\partial^2 F_j}{\partial z^2} - k^2 F_j = 0 \qquad (10.12)$$

$$\text{with } F_j \in \{E_j, H_j\},\ j \in \{x, y\}$$

The general solution of Eq. 10.12 is:

$$E_j = A_1 e^{-kz} + A_2 e^{kz} \qquad (10.13)$$

$$\text{with } j \in \{x, y\}$$

And after Eq. 10.2 and 10.6:

$$H_j = \frac{k \cdot (A_1 e^{-kz} - A_2 e^{kz})}{i\omega\mu} \qquad (10.14)$$

$$\text{with } j \in \{y, y\}$$

A_1 and A_2 are constant values. A_2 =0 resulting from the condition that the field must be finite for $z \rightarrow \infty$. Forming the quotient $Z_{xy} = E_x/H_y$ at the surface (z=0) which is called the impedance:

$$\frac{E_x}{H_y}\Big|_{z=0} = i\omega\mu / k = k / \sigma \tag{10.15}$$

In analogy:

$$Z_{xy} = \frac{E_y}{H_x}\Big|_{z=0} = -k / \sigma$$

where Zxy=-Zyx

Conductivity of the subsurface can also be obtained by measuring the electric and magnetic field components.

It is evident from Eq. 10.13 and 10.14 ($A_2 = 0$) that the amplitudes of the fields decrease exponentially with increasing depth. A commonly used criterion for the penetration of electromagnetic waves is the skin depth p, in which the signal amplitude is attenuated by 1/e:

$$p = \sqrt{\frac{\rho}{\pi \cdot f \cdot \mu}} \approx 500 \cdot \sqrt{\frac{\rho}{f}} \tag{10.16}$$

With p in m, ρ in Ωm and f in Hz. In general, there exists a unique transfer function (impedance tensor) between the horizontal electric and magnetic fields for a given angular frequency ω.

$$E = Z(\omega) \cdot H$$

$$\begin{bmatrix} E_x \\ E_y \end{bmatrix} = \begin{bmatrix} Z_{xx} & Z_{xy} \\ Z_{yx} & Z_{yy} \end{bmatrix} \cdot \begin{bmatrix} H_x \\ H_y \end{bmatrix} \tag{10.17}$$

For a layered, isotropic earth $Z_{xx} = Z_{yy} = 0$, the impedance tensor becomes a scalar number.

Apparent resistivity and phase values can be derived from the impedance tensor elements using the formula of Cagniard (1953):

$$\rho_{axy} = \frac{1}{\omega\mu} \cdot \left| Z_{yx} \right|^2 \tag{10.18}$$

$$\Phi_{xy} = \arctan\left[\frac{\mathrm{Im}(Z_{xy})}{\mathrm{Re}(Z_{xy})}\right]$$

Plots of the phases and the logarithmic apparent resistivities against the logarithmus of the decreasing or increasing signal frequency are commonly used to present radiomagnetotelluric studies.

For a 2D conductivity distribution with a strike direction chosen along the x-axis and therefore $Z_{xx} = Z_{yy} = 0$ and $Z_{xy} \neq Z_{yx}$, the transfer function is *composed* of two de-coupled principal components. They are determined by two linear and independent polarisation azimuths of the primary magnetic field:

- The component of the transfer function whose electrical field is along the strike of the structure is called the E-Polarisation or TE-mode (TE) of the transfer function.
- The component of the transfer function whose electrical field is normal to the strike of the structure is called the B-Polarisation or TM-mode (TM) of the transfer function.

For a 3D conductivity distribution, the distinction between E-Polarisation and B-Polarisation is no longer applicable.

For a 1D earth, the phases can be used to analyse the general conductivity distribution: phase values below 45° indicate a resistor at depth; phases above 45° indicate a conductor at depth.

In the radiomagnetotelluric method apparent resisitivity and phase values are measured in the frequency range from 10 kHz to 1 MHz (Fig 10.1). They will be interpreted by means of 1D and 2D inversion calculations in order to derive the conductivity distribution with depth. There are different types of RMT devices to estimate the impedance tensor and/or to measure directly the apparent resistivity and phase values. The next paragraph gives an overview about three commonly used instruments for near surface investigations.

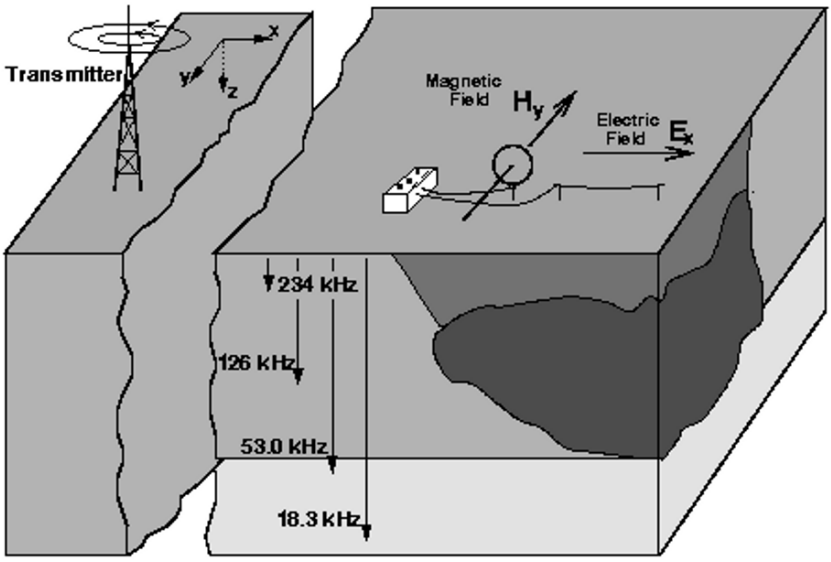

Fig. 10.1. The practical application of radiomagnetotellurics is to measure the electrical and magnetic fields. The apparent resistivities and phases are derived from using Eq. 10.18. A sounding information can be obtained by using different transmitters with different frequencies according to the skin depth of electromagnetic waves. Due to the skin effect, signals with lower frequency penetrate deeper into the subsurface

10.3 RMT Devices

First successful scalar RMT measurements in the frequency domain were carried out by using a system developed at the Centre of Hydrogeology at the University of Neuchâtel in Switzerland (CHYN). This device (Fig 10.2) weights 7 kg and only about 5 min. are required for measuring e.g. four preselected frequencies at one station. Scalar RMT means that only one polarization of the inducing horizontal magnetic field and only one polarization of the induced electric field are measured simultaneously thus providing either Z_{xy} and/or Z_{yx} data. The off diagonal elements of the impedance tensor are not measured. The device directly displayes apparent resistivities and phases. Large areas can be mapped quickly with this instrument. The component of the magnetic field is obtained by using an airloop, whereas the electric field is sampled by two grounded electrodes

with attached preamplifiers. A new version of this instrument allows measuring the electric field with a set of capacitive electrodes. The air loop has a diameter of 0.4 m and the distance between the electrodes can be chosen to be 1 or 5 m. The frequency range of this instrument is limited to 10 kHz - 240 kHz. No VLF transmitters are available below 10 kHz.

Fig. 10.2. The scalar RMT instrument developed by the Centre of Hydrogeology at the University of Neuchâtel (CHYN)

The recently developed tensor RMT technique has additional high resolution capabilities. Successful tensor RMT measurements were carried out by Pedersen and his group (Pedersen et al. 2005) using the 5-channel Enviro-MT system. In addition to the horizontal components of the magnetic and electric fields the vertical component of the magnetic field can be measured as well (Bastani 2001) allowing to estimate the full RMT impedance tensor and to estimate transfer function for the vertical magnetic field which is generally expressed as tipper or induction arrow data. All

electromagnetic signals between 10 - 250 kHz with a signal to noise ratio above 12 dB in the magnetic field are identified and stacked. The horizontal and magnetic noise levels are defined as the median filtered horizon of the ratio between the horizontal power and the estimated noise (Pedersen et al., 1994). Transfer functions are estimated in the frequency range between 10 - 250 kHz following Bastani and Pedersen (2001).The standard deviations are estimated, based on the signal to noise ratio of the inducing signals from the identified transmitters (Linde 2005).

Similar to the Enviro-MT system, another 4-channel tensor RMT system (RMT-F) was developed which records time series of the horizontal electric and magnetic fields. Compared to the other systems, the RMT-F device uses an extended frequency range from 10 kHz to 1 MHz simultaneously. (Fig. 10.3). The RMT transfer functions (e.g. expressed as apparent resisitivity and phases) can be derived by a statistical spectral analysis from the time series.

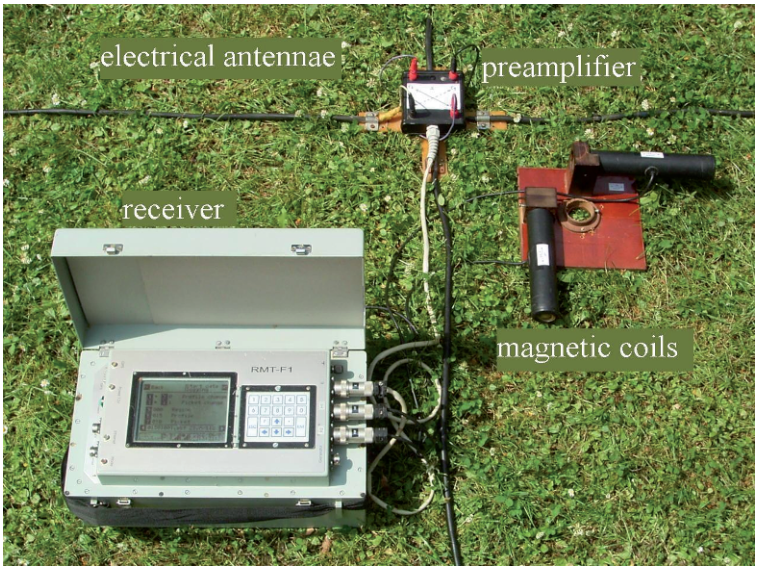

Fig. 10.3. The RMT-F system: Digital 4 channel receiver, electrical antennae, magnetic coils and E-field preamplifier

The RMT-F system consists of a receiver unit, two electrical antennae to observe the electric fields and two magnetic coils to measure the magnetic fields in perpendicular directions (Tezkan and Saraev 2007).

The measured time series contain all the frequencies from 10 kHz to 1MHz associated to powerful radio stations which are observable in the survey area. Time series can be transferred in the field to a laptop, so that they can be visualized. Auto and cross spectra densities can be calculated using a newly developed RMT data processing software (Tezkan and Saraev 2007). Specific radio transmitters are then easily identified in the power spectra as strong spectra lines in the narrow frequency interval (Fig. 10.4).

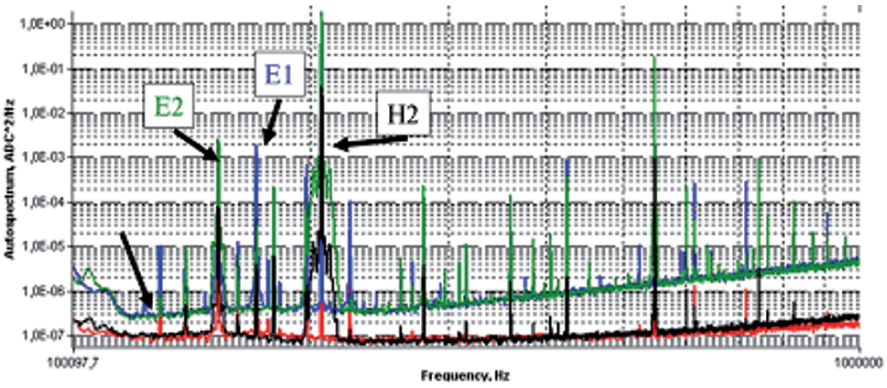

Fig. 10.4. Auto spectra calculated from time series of the horizontal electric and magnetic fields. H1 and H2 are showing the magnetic field in the northern and eastern direction. E1 and E2 are showing the corresponding electric fields in the eastern and northern directions respectively. The existing radio transmitters can easily be seen in the spectra as dominant spectra lines

The correct determination of the azimuth of radio transmitters is very important for a radiomagnetotelluric survey. All the azimuths of the radio transmitters available in the survey area can be viewed on a display. Then the user can define an azimuth range in which to select available transmitters of various frequencies and he can define a coherency level for the corresponding electric and magnetic field components. Those coherency values are typically chosen as 0.8. Apparent resistivity and phases can be then derived from the power and cross spectra.

RMT is an innovative and powerful technique for shallow subsurface investigations. However, the scalar and tensor devices are prototypes and there is no commercial tensor RMT system available so far. The key specification of the instruments are listed in Table 10.1.

Device	Type	Channels	Magnetic Field sensor	Electric Field sensor	Frequency range
RMT (CHYN)	Scalar (rho-app & phase)	H_x,E_y or H_y,E_x	Air loop or coil	2 electrodes or capacitive coupling	10 - 240 kHz
ENVIRO-MT	Tensor (time series)	H_x, H_y, H_z E_x, E_y	3 coils	4 electrodes	10 - 250 kHz
RMT-F	Tensor (time series)	H_x, H_y E_x, E_y	2 coils	4 electrodes or capacitive coupling	10 kHz - 1MHz

Table 10.1. Key specification of the three RMT instruments

10.4 Interpretation of RMT data

The distribution of radio transmitters in Europe is dense enough for using their plane waves to estimate RMT transfer functions in the 10kHz -1MHz band (Pedersen et al. 2006). In addition, displacement currents can be neglected for normal resitivity distribution, so that the well developed 2D inversion software of magnetotellurics (MT) can be directly applied on RMT data. (Smith and Booker 1991, Siripunvarapon and Egbert 2000, Mackie et al. 1997).

The application of 2D inversion algorithms is the standard interpretation of RMT data to derive the conductivity distribution of the subsurface.

The 2D inversion of RMT data is however ill posed and a regularisation procedure must be implemented (Mackie et al. 1997) for example use of Tikhanov´s method which defines a regularized solution of the inverse problem as a model m that minimizes the objective function:

$$S(m) = (d - F(m))^T R_{dd}^{-1} (d - F(m)) + \tau \left\| L(m - m_0) \right\|^2 \qquad (10.19)$$

Where d = observed data vector, F = forward modelling operator, m = unknown model vector, R_{dd} = error covariance matrix, m_0 = a priori model, τ = regularisation parameter. (Mackie et al. 1997) use a Laplacian operator ($L = \Delta$):

$$\left\| L(m - m_0) \right\| = \int (\Delta(m(x) - m_0(x)))^2 \, dx \tag{10.20}$$

An important parameter which influences the result of the inversion is the regularisation parameter τ. L curve criteria (e.g. Hansen and O'Leary 1993) can be used to determine its value. Mackie et al. (1997) suggested to choose the value of τ in such a way, that the RMS error:

$$RMS = \sqrt{(d - F(m)^T \cdot R_{dd} \cdot (d - F(m)) / N} \tag{10.21}$$

is between 1 and 1.5. N is the number of the data points. The 2D inversion can be realized separately using the RMT data associated with the TE or TM data. A joint inversion can also be carried out using both TE and TM data. Pedersen et al. (2005) also suggests using the determinant of the impedance tensor as input for a 2D inversion to suppress 3D effects.

In addition to 2D inversions, 3D inversions of RMT can be realized which is, however, a very time consuming procedure and cannot be applied in a standard way. In the following section, selected RMT case studies will be shown demonstrating the efficiency of the 2D and 3D inversion of the observed RMT data.

10.5 Case studies

Successful RMT studies have been reported in the literature to study spatial changes in lithology (Turberg et al. 1994) to explore waste sites and contaminated soils (Tezkan et al. 2000, 2005) and to map the depth of bedrock (Beylich et al. 2004).

Well developed and tested 3D inversion software allows a quantitative interpretation of RMT data. RMT case studies for a waste site exploration (Newman et al. 2003) and for the study of contaminated soil (Tezkan et al. 2005) are presented in the following.

10.5.1 Contaminated site exploration

Scalar RMT measurements were carried out on a contaminated area close to the Brazi refinery in Romania (Fig.10.5) in order to detect a 1m thick oil layer expected at 3 m depth (Tezkan et al. 2005). Fig. 10.5 also shows the variation of the thickness of the hydrocarbon contaminants as derived from boreholes. Fig. 10.6 shows a cross section, which is also indicated in Fig. 10.5.

Radio transmitters broadcasting in the frequency range from 10 kHz to 250 kHz were selected to observe apparent resistivity and phase data associated with TE and TM modes. They were located parallel and perpendicular to the assumed strike direction of the contamination plume (Fig. 10.6).

Fig. 10.7 shows the distribution of apparent resistivity and phase for a selected frequency. The apparent resistivities decrease with increasing distance from the refinery. On the other hand, relative small phase variations were observed for this frequency in the whole area. The variation of the conductivity as a function of depth can be seen by considering all apparent resistivity and phase values for different frequencies.

Fig. 10.8 shows the frequency dependence of apparent resistivities and phases at selected stations. The location of the stations is indicated in Fig. 10.7. In addition, apparent resistivity and phase curves observed outside of the contaminated area are shown.

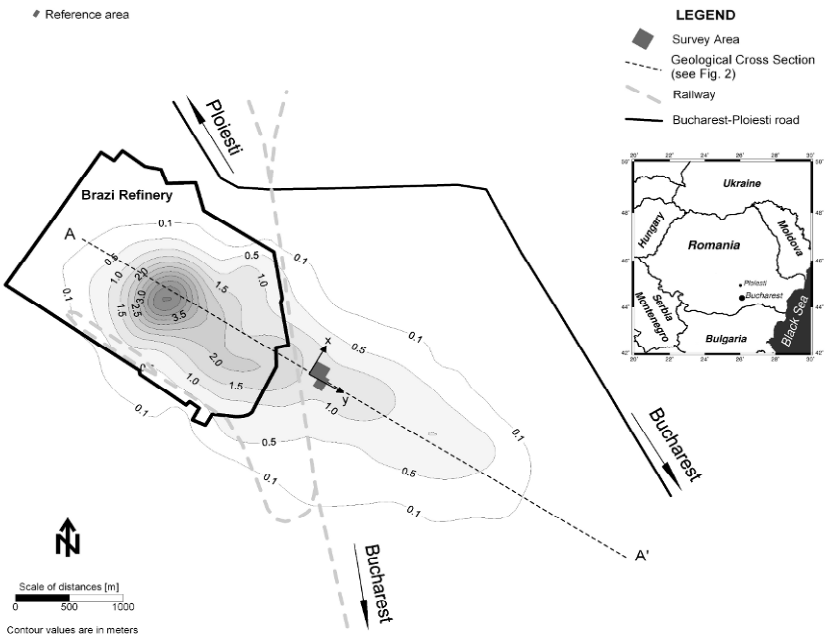

Fig. 10.5. Location of the RMT measurements on the contaminated survey area. The contour lines indicate the variation in the thickness of the hydrocarbon contamination above the groundwater table in meters. (Tezkan et al. 2005)

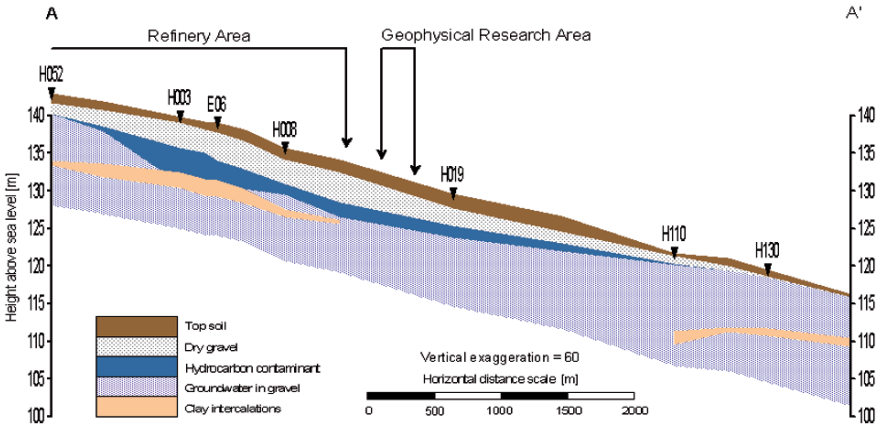

Fig. 10.6. Geological cross section in NW-SE direction derived from the boreholes in the survey area. The location of the geological section is indicated in Fig. 10.5. Triangles mark the selected boreholes (Tezkan et al. 2005)

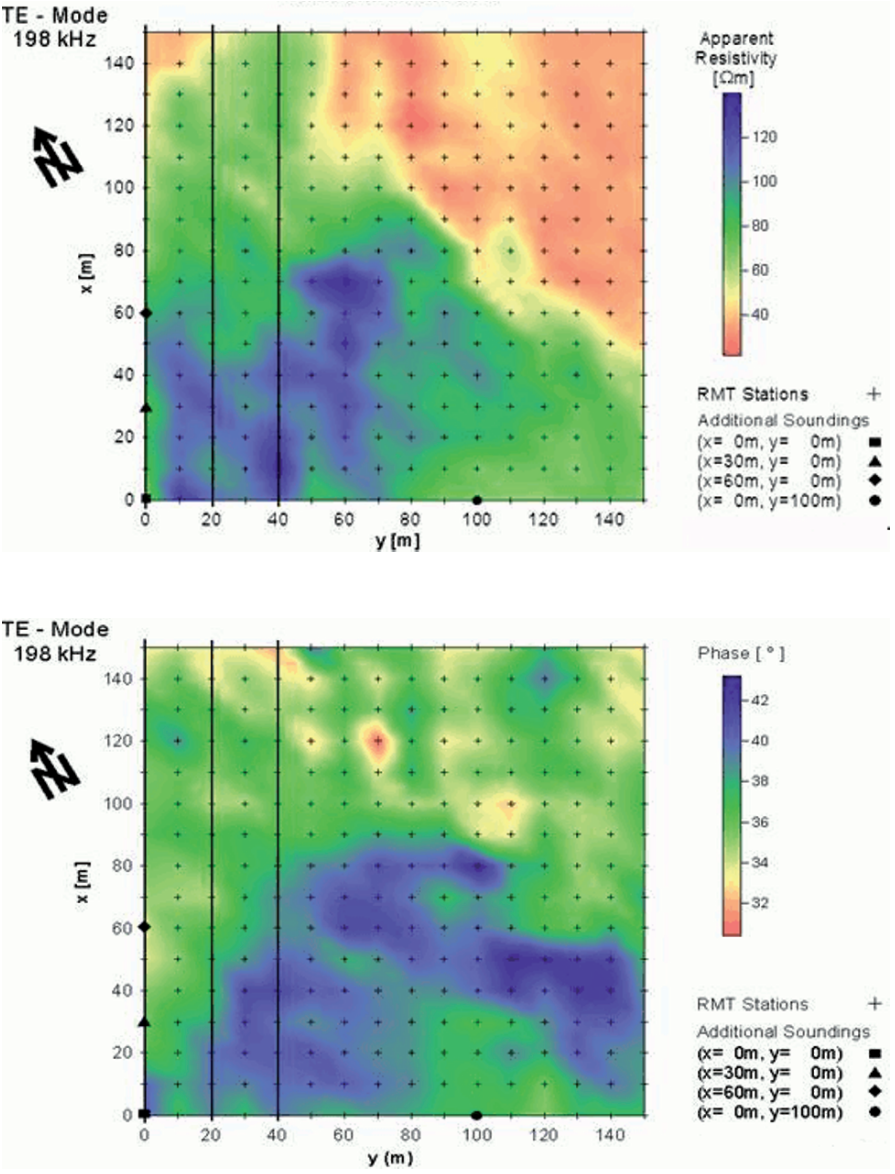

Fig. 10.7. Spatial distribution of the apparent resistivity and phase for the frequency 198 kHz. The markings indicate the location of the RMT stations and additional RMT sounding points (Tezkan et al. 2005)

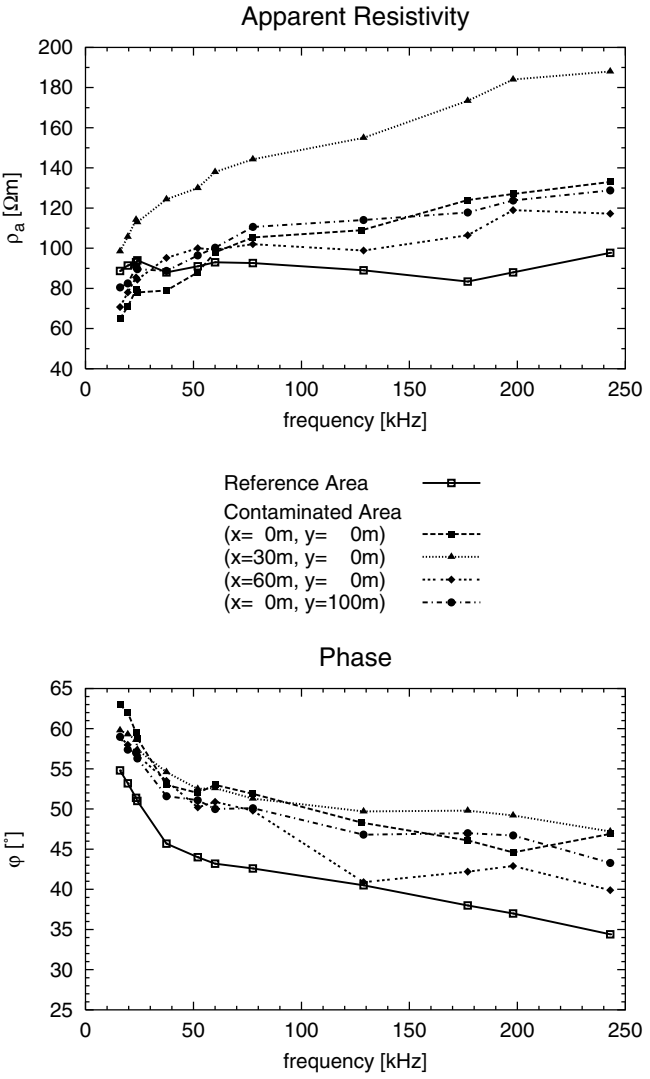

Fig. 10.8. Frequency dependence of apparent resistivities and phases value at different locations in the contaminated area and in the reference field (Tezkan et al. 2005)

The apparent resistivity in the contaminated area increased with increasing frequency while the phase decreased in both the reference and the contaminated area. Sounding data from the reference field show that the apparent resistivity was almost frequency independent. The significant difference in the apparent resistivities of the reference and contaminated

areas may be interpreted as an indication of contamination at shallow depth, since the apparent resistivities of the contaminated area increases with increasing frequency. On the other hand, the apparent resistivity of the reference field is almost constant for all frequencies.

Fig. 10.9 shows 2D inversion results for the profiles y = 0, 20 and 40 (Fig. 10.7). As expected from the observed data, there is a resistive layer below a conductive surface layer from 3 - 13 m. Beneath the two layers a conductive half space associated with a marl layer was observed and confirmed by borehole results. A highly resistive lens detected inside the middle resistive layer can be associated with hydrocarbon contamination. Observations at a large number of boreholes existing in this area show relative thick (≈ 1m) oil layer at a depth of 5 m caused by many accidents in the refinery.

In general RMT is effective in monitoring pollution but ineffective in monitoring organic liquids, the method is very effective if the targets are conductive (e.g.) waste sites as the following case study shows.

The experiment presented in this case study shows a possible application of the RMT technique for the detection of oil contamination in the earth.

10.5.2 Waste site exploration

A RMT field data set observed over a buried waste site near Cologne / Germany has been interpreted successfully by using a 3D inversion scheme (Newman et al. 2003). Fig.10.10 illustrates a surface map of the site where the solid line indicates the border of the waste site. Fig. 10.10 also shows the location of the 320 RMT stations. Due to logistical reasons not all the measurement profiles cross the boundary of the pit. Every measurement used in scalar mode eight frequencies to cover the range between 234 kHz to 18.3 kHz.

Fig. 10.11 gives an overview of the lateral distribution of the apparent resistivity and phases for a selected frequency of 234 kHz. The waste is indicated when the apparent resistivity ρ_a is less then 40 Ωm. The lateral border of the waste site with respect to undisturbed geology (ρ_a >100 Ωm) can only be seen in the southern part of the area. The phase map shows the crossing of the undisturbed geology to the waste pit with an increase in phase from 35 degrees to more than 55 degrees.

The field data sets was inverted using 3D inversion schemes (Newman et al 2003).First of all, a background geological model of the site was constructed which served as a starting model for the 3D inversion of the field data (Newman et al. 2003). This two layered model consists of a 200 Ωm

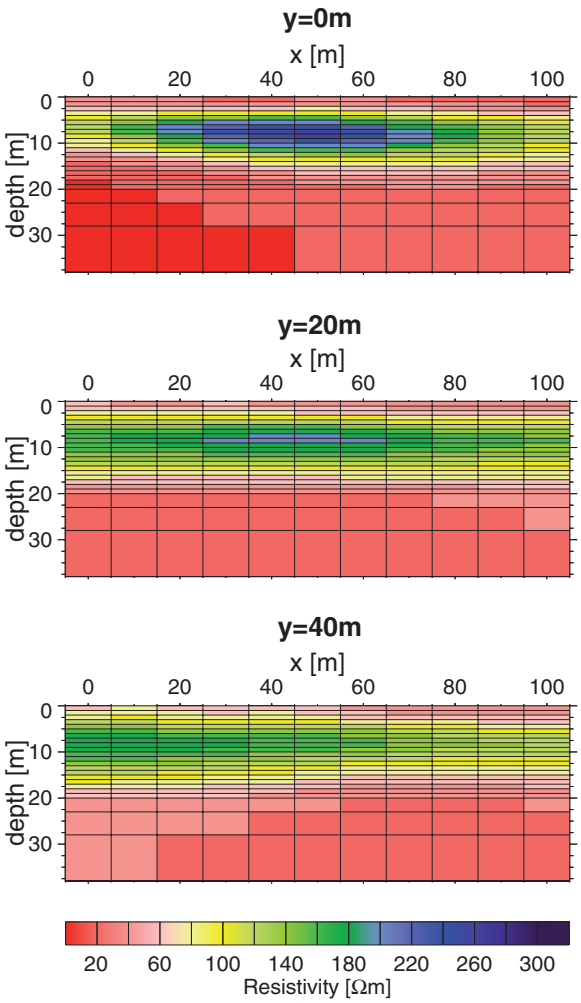

Fig. 10.9. 2D resistivity distribution below the profiles y=0m, 20 m and 40 m (Tezkan et al. 2005)

gravel layer, 20 m thick and a 25 Ωm basal conductor. This background model was derived from the 2D inversion of RMT measurements collected along the reference profile (Fig. 10.10). Fig. 10.12 shows the 3D inversion results using a two layered starting model based on the background geology. A sharper image of the waste pit is obtained. The base of the pit is derived to be near 13 m and is good agreement with borehole data. The result of the 3D inversion can be also visualized in 3D spatial dimension. The pit volume is estimated to be 603,600 cubic meters assuming $\rho < 50$ Ωm.

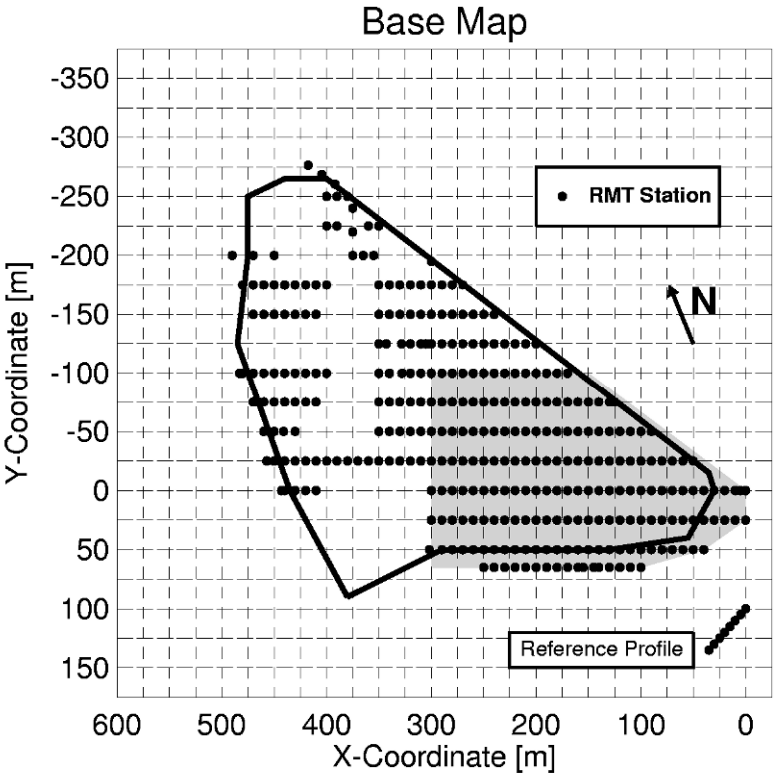

Fig. 10.10. Base map of the survey area. The black line indicates the boundary of the pit. The grey area shows the region that corresponds to the apparent resistivity and phase maps in Fig. 10.11 (Newman et al. 2003)

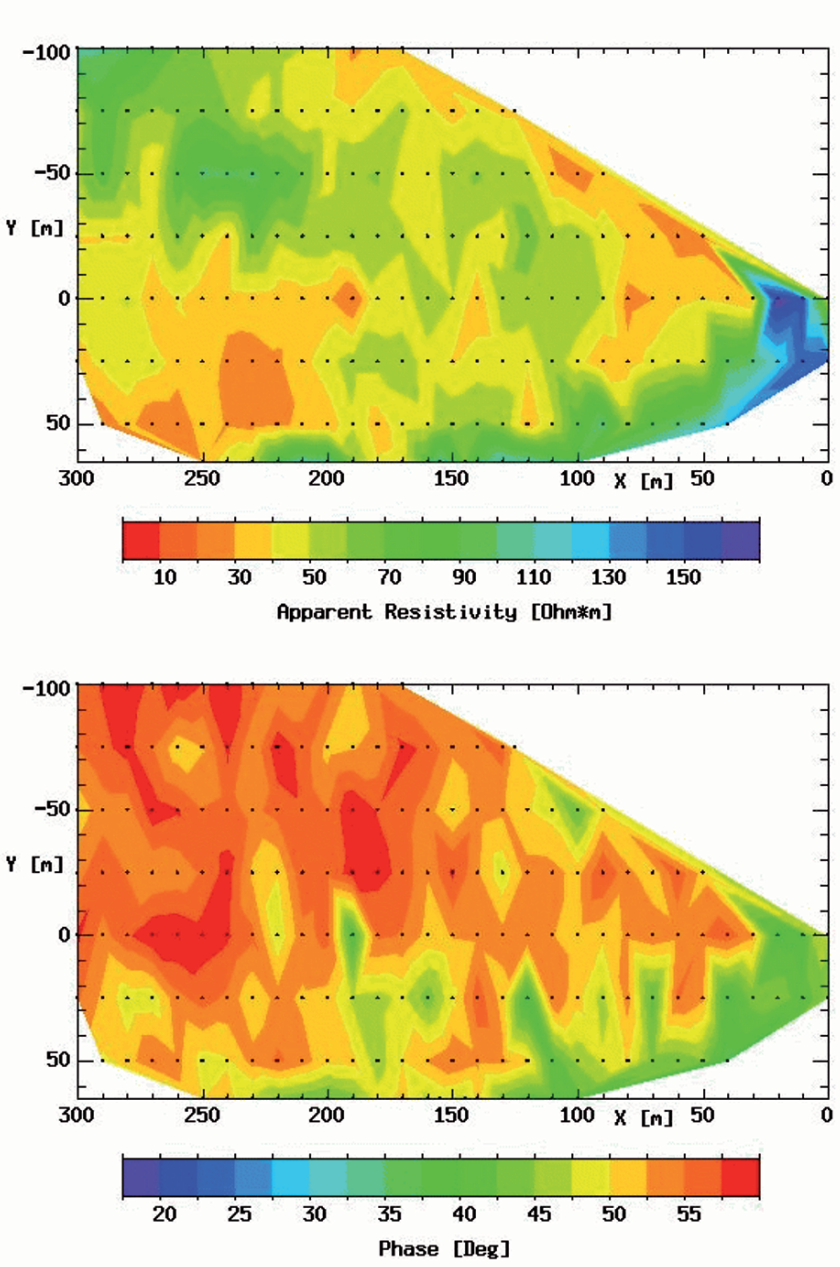

Fig. 10.11. Apparent resistivity and phase maps over a part of the survey area, corresponding to the grey area in Fig. 10.10 (Newman et al. 2003)

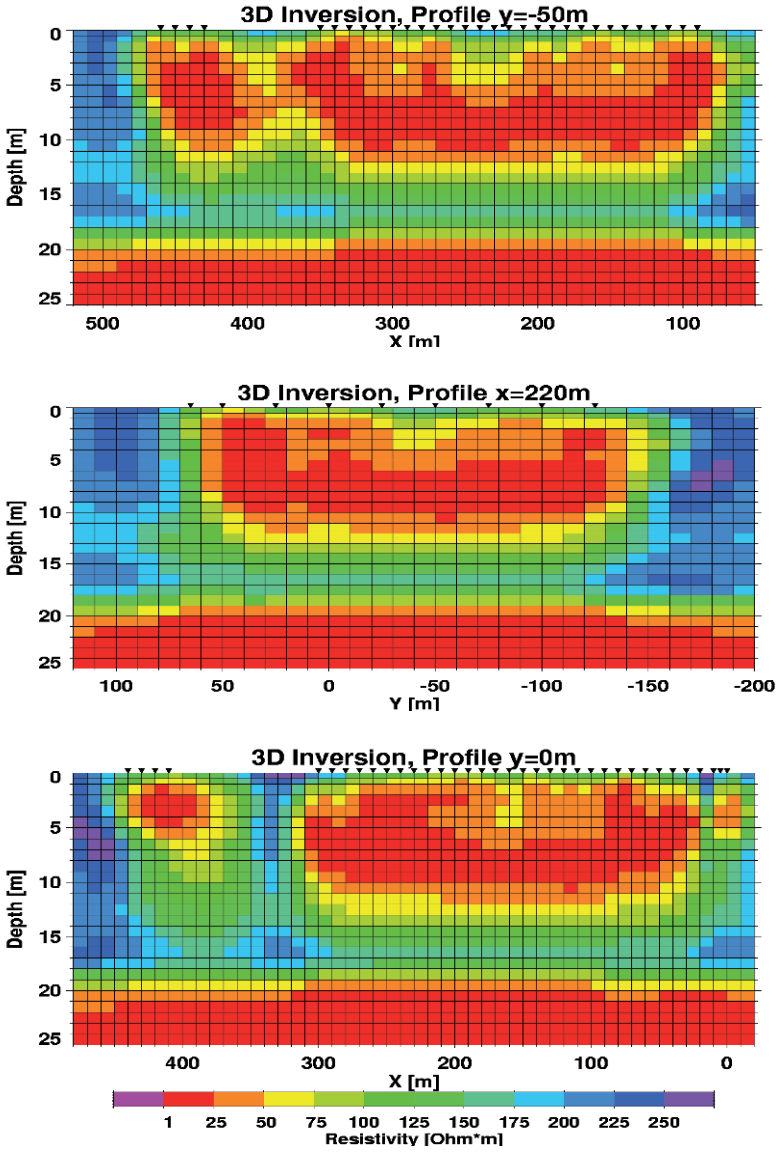

Fig. 10.12. 3D inversion results using a two layered model based on the background geology. The pit can be clearly seen in the three images of selected profiles as a good conductive body. (Newman et al. 2003)

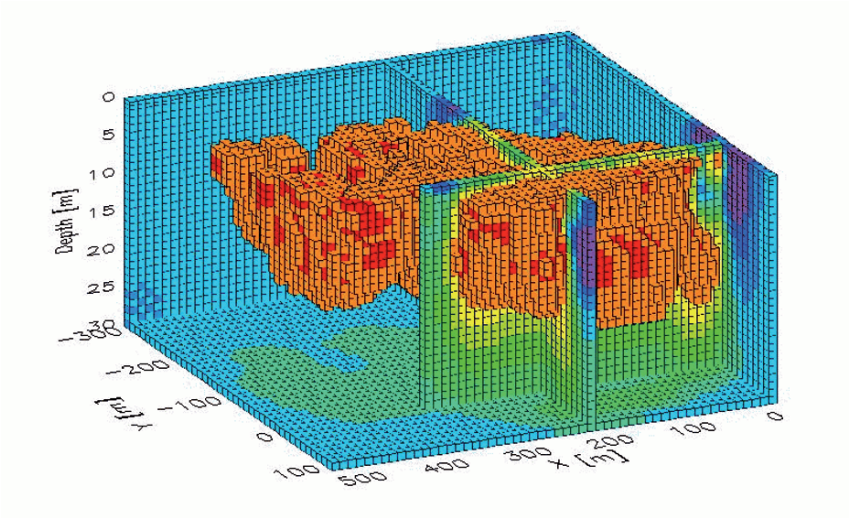

Fig. 10.13. 3D rendering of the waste pit. Resistivities greater than 50 Ωm have been rendered invisible.(Newman et al. 2003)

10.6 References

Bastani M; Pedersen LB (2001) Estimation of magnetotelluric transfer functions from radio transmitters. Geophysics 66:1038-1051

Bastani M (2001) EnviroMT - a new controlled source radiomagnetotelluric system. PhD dissertation , Uppsala Univ., Uppsala, Sweden

Bechtel T., Bosch F., Gurk, M. (2007) Geophysical Methods, in Nico Goldscheider & David Drew (eds.): Methods in Karst Hydrogeology, ISBN: 9780415428736, 276 pp

Beylich A.A, Kolstrup E, Thyrsted, Linde N, Pedersen LB, Dynersius L (2004) Chemical denudation in arctic-alpine Latnjavagge in relation to regolith as assessed by radio magnetotelluric geophysical profiles. Gemorphology 57:303-319

Cagniard L (1953) Basic theory of magnetotelluric method of geophysical prospecting. Geophysics 18:605-635

Hansen PC, O´Leary DP (1993) The use of L-curve in the regularisation of discrete ill-posed problems. SIAM Journal of Scintific Computing 14:2003

Linde N (2005) Characterisation of hydrogeological media using electro-magnetic geophysics. PhD thesis, Uppsala Univ., Sweden

Linde N; Pedersen LB (2004) Characterization of a fractured granite using radiomagnetotelluric data. Geophysics 69:1155-1165

Mackie R, Rieven S; Rodi W (1997) Users manual and software documentation for two dimensional inversion of magnetotelluric data. Massachusetts Institute

of Technology, Earth Resources Laboratory, Cambridge, Massachusetts 02139
McNeill JD (1990) Use of Electromagnetic Methods for Groundwater Studies. In: Ward SH (ed) Geotechnical and Environmental Geophysics, vol 1. Soc Expl Geophys, Tulsa, pp 191 – 218
Nabighan MN (1987) Electromagnetic methods. In: Applied Geophysics, Vol.1, Tulsa, Society of Exploration Geophysicists
Newman GA; Recher S; Tezkan B, Neubauer FM (2003) 3D inversion of a scalar radiomagnetotelluric field data set. Geophysics 68:791-802
Nobes DC (1996) Troubles waters. Enviromental application of electric and electromagnetic methods. Surveys in Geophysics 17:393-454
Pedersen LB, Bastani M, Dynesius L (2006) Some characteristics of the electromagnetic field from radio transmitters in Europe. Geophysics 71:279-284
Pedersen LB, Bastani M, Dynesius L. (2005) Ground water exploration using combined controlled source and radiomagnetotelluric techniques. Geophysics 70:608-615
Pedersen LB, Qian W, Dynesius L, Zhang P (1994) An airborne tensor VLF system - from concept to realisation. Geophys. Prospection 42:863- 883
Pellerin L (2002) Application of electric and electromagnetic methods for environmental and geotechnical investigation. Surveys in Geophysics 23:101-132
Persson L; Pedersen B (2002) The importance of displacement currents in RMT measurements in high resistivity environments. Journal of Applied Geophysics 51:11-20
Siripunvarapon W, Egbert G (2000) An efficient data-subspace inversion method for 2D magnetotelluric data. Geophysics 65:791-803
Smith JT, Booker JR (1991) Rapid inversion of two and three dimensional magnetotelluric data. Journal of Geophysical Research 96:3905-3922
Telford WM, Geldart L, Sheriff RE, Keys DA (1990) Applied Geophysics, 2nd Edition, Cambridge -University Press, Cambridge
Tezkan B, Saraev A (2007) A new radiomagnetotelluric device for environmental geophysics operating in the frequency range from 10kHz-1MHz. Extended abstract, 20. SAGEEP meeting, Denver Colorado, USA
Tezkan B, Georgescu P, Fanzi U (2005) A radiomagnetotelluric survey on an oil-contaminated area near the Brazi Refinery, Romania. Geophysical Prospecting 53:311-323
Tezkan B, Hoerdt A, Gobashy M (2000) Two dimensional magnetotelluric investigation of industrial and domestic waste sites in Germany. J. Appl. Geophys. 44:237-256
Tezkan B (1999) A review of environmental applications of quasi-static electromagnetic techniques. Surveys in Geophysics 20:279-308
Turberg PI, Barker R (1999) Joint application of radio-magnetotelluric and electrical imaging surveys in complex subsurface environments. First Break 14
Turberg PI; Müller I; Flury F (1994) Hydrogeological investigation of porous environments by radiomagnetotelluric resistivity (RMT-R 12-240 kHz). J.Appl. Geophys. 31:133-143